Velocity and Timing of Multiple Spherically Converging Shock Waves in Liquid Deuterium

T. R. Boehly, V. N. Goncharov, W. Seka, M. A. Barrios, P. M. Celliers, D. G. Hicks, G. W. Collins, S. X. Hu, J. A. Marozas, and D. D. Meyerhofer

Phys. Rev. Lett. **106**, 195005 — Published 13 May 2011

DOI: 10.1103/PhysRevLett.106.195005

The velocity and timing of multiple spherically-converging shock waves in liquid deuterium

T. R. Boehly,[1] V. N. Goncharov,[1] W. Seka,[1] M. A. Barrios,[1] P. M. Celliers,[2]

D. G. Hicks,[2] G. W. Collins,[2] S. X. Hu,[1] J. A. Marozas[1], D. D. Meyerhofer[1,3]

[1]Laboratory for Laser Energetics, University of Rochester, 250 East River Road,

Rochester, NY 14623-1299

[2]Lawrence Livermore National Laboratory, Livermore, CA

[3]Departments of Mechanical Engineering and Physics, University of Rochester

ABSTRACT

The fuel entropy and required drive energy for an inertial confinement fusion (ICF) implosion is set by a sequence shocks that must be precisely timed to achieve ignition. This Letter reports measurements of multiple, spherical shock waves in liquid deuterium that facilitate timing ICF shocks to the required precision. These experiments produced the highest shock velocity observed in liquid deuterium (U_S = 135 km/s at ~2500 GPa) and also the first observation of convergence effects on the shock velocity. Simulations model the shock-timing results well when a nonlocal transport model is used in the coronal plasma.

Inertial confinement fusion (ICF) target designs use a sequence of shocks to compress the shell and fuel assembly before they implode [1]. The fuel entropy is controlled by optimizing the strength and timing of these shocks. The goal is to maintain the internal pressure of the fuel to ~1 to 2 times its Fermi-degenerate pressure to minimize the required driver energy. To achieve these optimal conditions, the four shocks must merge in a precise sequence at the inner surface of the fuel layer [2,3]. The experimental program for ICF ignition [4] on the National Ignition Facility (NIF) [5] includes a series of tuning experiments to verify shock strength and timing as a method to achieve optimal drive conditions for hohlraum-driven ignition targets [3]. This Letter reports on experiments that measure the velocity (strength) and timing of multiple, converging shock waves *inside* spherical targets filled with liquid (cryogenic) deuterium.

These experiments develop a shock-timing technique for ignition targets and validate simulations of direct-drive ICF targets [6]. The development was successful and this technique will be directly applied to full-scale experiments to tune hohlraum-driven ignition targets on the NIF [7]. To model these experiments, the simulations incorporated a nonlocal model [6] to treat heat conduction in the coronal plasma. These simulations model shock velocity and timing quite well, providing confidence in the hydrodynamic codes used to design direct-drive ICF targets for OMEGA and the NIF.

The experiments were performed on OMEGA—a 60-beam, 351-nm laser designed to directly drive spherical-target implosions with high-irradiation uniformity [8]. Multiple laser pulses produce up to four distinct shocks with velocities ranging from 20 to 130 km/s. These are the first experiments to detect and time multiple, spherically converging shock waves in liquid deuterium. They are the highest shock velocities

(>130 km/s) reported in liquid deuterium and represent the first reported observation of the effects of spherical convergence on shock velocity.

In a direct-drive ICF implosion, the initial shock waves are produced by short laser pulses preceding the main pulse that drives the implosion [9]. Short individual pulses are desirable because they are impulsive on hydrodynamic time scales. As a result, only the energy contained in the pulse matters, not its temporal shape. Moreover, individual laser pulses provide discrete drive events that are easily tuned for optimizing the shock timing.

The OMEGA laser produced a sequence of up to four shocks, whose strength and timing were designed so that the later, stronger shocks overtake earlier weaker ones to produce multiply shocked deuterium. The shocks ultimately coalesced about 200 μm into the deuterium, forming a single strong shock that converges toward the center of these targets. The shock velocities and the times of these mergers are measured with high precision using time-resolved velocity interferometry [10] and streaked optical pyrometry [11]. The shock velocity and timing are measured to better than the ~1% and ±50-ps precision required for ignition targets.

The velocity interferometery system for any reflector (VISAR) [10] detects the Doppler shift of an optical (532-nm) probe beam that reflects off the shock front. At the pressures studied here, the shocks have a reflectance greater than 30% [12]. To provide diagnostic access to those shock waves, the spherical targets were fitted with a diagnostic cone similar to those used in the fast-ignition concept [13]. The targets are described in Ref. [7] and are shown schematically in Fig. 1. The 900-μm-diam, 10-μm-thick CD spherical shell and the cone were filled with liquid deuterium; VISAR observed the

shocks on the *inside* of the shell through an aperture in the end of the cone. The sphere was irradiated by 36 OMEGA beams on the hemisphere opposite the line of sight of VISAR. The beams were fitted with the same SG4 distributed phase plates [14] used for the 60-beam ICF implosion experiments [15]. The experiments reported here are surrogates for the shock-transit portion of a spherically symmetric ICF implosion. The liquid deuterium (replacing the deuterium–tritium ice layer) provides an extended and uniform medium within which the shocks propagate. In addition to VISAR, a streaked optical pyrometer (SOP) [11] observes the optical self-emission from the shocks in the deuterium.

Figure 2(a) shows VISAR data for a three-shock experiment (shot 59533) driven by three ~100-ps laser pulses (at 0, 1, and 2 ns) as shown in white in the image. The VISAR record is a 1-D image (vertical axis) of the target that is streaked in time (horizontal axis). Imposed on that image is a series of fringes whose vertical position (fringe phase) is proportional to the shock velocity. The image in Fig. 2(a) is a view of the shocks in the deuterium within the shell observed through the aperture in the re-entrant cone. The experiment is arranged so these shock waves spherically converge along the VISAR axis. VISAR tracks this convergence until the shock impacts the front of the cone, which is 200 μm from the inside of the sphere.

Before $T = 0$, the fringes in Fig. 2(a) are horizontal because there is no shock or movement in the target. At $T = 0$ the signal disappears because the VISAR probe is absorbed by the CD shell which is photoionized by x rays from the laser-produced plasma. After the shock transits the CD and reaches the deuterium (which remains transparent), the VISAR signal returns and the fringes abruptly shift in response to the

shock velocity in the deuterium. At that time, the shock produced by the short pulse is unsupported and is decelerating; the resulting VISAR fringes exhibit curvature in time.

At 2.4 ns, the shock produced by the second laser pulse (at ~1 ns) overtakes the first shock. (VISAR does not detect the second shock until it overtakes the first, because the first shock is reflective and opaque; it blocks VISAR's view.) At that point, the coalesced shock (first and second shocks) is stronger and has a higher velocity; VISAR detects this sudden increase in velocity as a jump in fringe position. Since this shock is also unsupported, it decelerates as it travels through the deuterium and the fringes slope downward. (The decay rate of this second shock is different than that of the first because the rarefaction wave that produces it now encounters double-shocked deuterium.) At 2.9 ns, the shock from the third pulse (at 2 ns) overtakes that coalesced shock and another jump in velocity occurs. This final shock is also unsupported and begins to decay, producing a downward motion of the fringes in time. At about 4 ns the fringes turn upward, indicating acceleration. In the time 2.9 to 5 ns, the third shock started at ~90 km/s, decayed to 74 km/s and then accelerated back to ~90 km/s before the signal was lost. This increase in velocity is a result of the pressure increase produced by spherical convergence [16]. This is the first reported observation of shock-velocity increase due to spherical convergence in deuterium. Lastly, at ~4 ns the shock impinges on the face of the cone, producing a disturbance that propagates into the cone aperture and the VISAR line of sight. This produces the brighter signal (without fringes) that moves toward the center of the image as the disturbance fills the aperture at ~5 ns.

Figure 2(b) shows the SOP data acquired simultaneously with the VISAR data in Fig. 2(a). This is a color-scaled image (vertical axis) of the self-emission intensity

streaked in time (horizontal axis). The solid black line through the image is a plot of the intensity (horizontal line-out) that represents the temporal profile of shock brightness (temperature), which is proportional to the velocity. Note that in response to the various shocks, the SOP intensity decays and jumps in a fashion similar to the VISAR data providing an independent measure of shock strength and timing.

For ignition targets, shock waves must sequentially merge at the desired time with a precision of ±50 ps. In the VISAR data in Fig. 2, the shock mergers cause fringe jumps that occur over two of the 10.6-ps pixels (i.e., in ~22 ps). Calibration techniques and the temporal fiducials on these data allow one to calibrate the streak camera sweep rates to better than 1% precision. Together, they provide the necessary precision to time shock waves on OMEGA and the NIF to the ±50 ps required for ignition targets.

A direct-drive ICF implosion on OMEGA has a long (~1-ns) fourth pulse that drives the target implosion. This pulse is more intense and has significantly higher energy than the individual ~100-ps pulses preceding it. For shock-timing experiments, x rays from that fourth drive pulse can be sufficiently intense to photoionize the quartz window at the end of the VISAR cone, preventing VISAR measurements. The inset in Fig. 3 shows the VISAR signal from a four-pulse experiment where the (final) drive-pulse intensity was reduced to measure all four shocks using VISAR. The features of the data are similar to those in Fig. 2(a): the merger of the second shock with the first is evident at 1.9 ns; then at 2.4 ns the third shock merges with the first two. At 3 ns the fourth shock from the main drive pulse (which started at 2 ns) overtakes the three merged shocks. Soon after, the VISAR signal disappears. This is because at the high pressure (and temperature) of this fourth shock, the self-emission is sufficiently high to photoionize the

unshocked deuterium ahead of it absorbing the VISAR probe beam. [Note that the signal from the cone face (bottom of inset image) persists beyond 4 ns. This indicates that loss of VISAR signal from the fourth shock is not due to blanking of the window.]

Figure 3 shows the velocity profile deduced from VISAR (solid), showing shock velocities of 50, 56, 72, and 130 km/s for each of the four shocks. The latter velocity corresponds to a pressure of 2500 GPa in the deuterium; this is the highest pressure that deuterium shock velocity has been reported. Ignition targets on the NIF will have the first three shock velocities in the range of 20, 40, and 70 km/s. These results show that shocks of those strengths in deuterium can readily be observed and timed using this technique.

For direct-drive ICF target designs, radiation–hydrodynamic codes have long used a heuristic *flux-limiter* model [17] to simulate the reduced flux of energy from the corona, where laser energy is deposited, to the ablation surface, where pressure is applied to the target. To simulate many ICF experimental results, the heat flux must be limited to ~6% of that predicted by the Spitzer–Härm free-streaming limit, primarily in regions of steep temperature gradients such as near the ablation front. In recent direct-drive experiments with laser intensities above 3×10^{14} W/cm^2, measurements of absorption, acceleration, and scattered light were not well modeled using the flux limiter [18,19] and required a nonlocal transport code to properly simulate the data. This is also true for the shock-velocity measurements.

Figure 3 shows the shock-velocity profile predicted by *LILAC* (dashed) when a nonlocal model is used [15]. Simulations with a flux limiter typically underestimated the velocity of the first shock by as much as 10%, and as a result, the timing of subsequent shock mergers is poorly predicted. This is because early in time, when the first pulse

interacts with solid target, the density scale length is very short near the critical density where the majority of laser light is absorbed. In the flux-limit model, the classical Spitzer flux is replaced with 6% of the free-stream limit in a narrow region near this surface. This abruptly occurs in a few zones and produces a non-physical jump in the electron density near the critical surface; this alters the density scale length in the corona, leading to reduced absorption of laser light. The nonlocal treatment eliminates this jump, resulting in a more-accurate simulation of the corona yielding higher laser coupling and a stronger first shock, in better agreement with experimental data.

Figure 3 shows how both the shock velocities and the merger times are well modeled by the simulation. Proper treatment of the electron transport is essential to correctly model these plasmas and predict shock timing. That the simulations accurately predict the first shock velocity indicates that the codes adequately treat the plasma initiation. Similarly, the good agreement with the subsequent shock velocities indicates the expansion of the coronal plasma and the interaction of later pulses with that preformed plasma are well modeled. That the predicted velocities and merger times agree with experiments indicates that the material properties (equations of state for CH and deuterium) used in the codes are adequate. Obtaining good simulation of these data depended greatly on locating the target to within ~30 □m of the desired position. This assured that the irradiation uniformity and intensity were as designed and could be properly simulated.

Multiple, converging shock waves have been observed in spherical cryogenic targets directly irradiated with laser pulses. The fourth shock produced a shock velocity of 135-km/s in cryogenic deuterium. This is the highest reported shock velocity in

deuterium and corresponds to a pressure of ~2500 GPa (25 Mb). This is also the first measurement of converging shock velocity that exhibited a pressure (velocity) increase due to spherical convergence.

These experiments are the first to time multiple, spherically converging shock waves in liquid deuterium; they demonstrate the ability to time and control shock waves to the precision needed for ignition experiments. The observed deuterium shock velocities were similar to and greater than those required for the initial phase of an ignition target on the NIF. This technique will be directly applied to full-scale experiments to tune the laser pulse for hohlraum-driven ignition targets on the NIF.

To properly simulate these results, the hydrodynamic codes need to account for heat transported by energetic electrons in thermal distribution. At high intensities, the initial plasmas produced by short (100-ps) pulses have steep density and temperature gradients, which the standard flux-limiter models do not properly treat. When a nonlocal thermal transport model is used, the shock velocities and timing are better modeled by the simulations. The ability to simulate these experimental results provides confidence in the hydrodynamic codes used to design direct-drive ICF targets for OMEGA and the NIF.

ACKNOWLEDGMENT

This work was supported by the U.S. Department of Energy Office of Inertial Confinement Fusion under Cooperative Agreement No. DE-FC52-08NA28302, the University of Rochester, and the New York State Energy Research and Development Authority. The support of DOE does not constitute an endorsement by DOE of the views expressed in this article.

REFERENCES

[1] J. D. Lindl, *Inertial Confinement Fusion: The Quest for Ignition and Energy Gain Using Indirect Drive* (Springer-Verlag, New York, 1998).

[2] D. H. Munro *et al.*, Phys. Plasmas **8**, 2245 (2001).

[3] D. H. Munro *et al.*, Bull. Am. Phys. Soc. **51**, 105 (2006).

[4] B. A. Hammel and the National Ignition Campaign Team, Plasma Phys. Control. Fusion **48**, B497 (2006).

[5] E. I. Moses, Fusion Sci. Technol. **54**, 361 (2008).

[6] V. N. Goncharov *et al.*, Phys. Plasmas **15**, 056310 (2008).

[7] T. R. Boehly *et al.*, Phys. Plasmas **16**, 056302 (2009).

[8] T. R. Boehly *et al.*, Opt. Commun. **133**, 495 (1997).

[9] V. N. Goncharov, in *Laser-Plasma Interactions*, edited by D. A. Jaroszynski, R. Bingham and R. A. Cairns, Scottish Graduate Series (CRC Press, Boca Raton, FL, 2009).

[10] P. M. Celliers *et al.*, Rev. Sci. Instrum. **75**, 4916 (2004).

[11] J. E. Miller *et al.*, Rev. Sci. Instrum. **78**, 034903 (2007).

[12] P. M. Celliers *et al.*, Phys. Rev. Lett. **84**, 5564 (2000).

[13] R. Kodama *et al.*, Nature **412**, 798 (2001).

[14] Y. Lin, T. J. Kessler, and G. N. Lawrence, Opt. Lett. **20**, 764 (1995).

[15] V. N. Goncharov *et al.*, Phys. Rev. Lett. **104**, 165001 (2010).

[16] Von G. Guderley, Luftfahrtforschung **19**, 302 (1942).

[17] R. C. Malone, R. L. McCrory, and R. L. Morse, Phys. Rev. Lett. **34**, 721 (1975).

[18] W. Seka *et al.*, Bull. Am. Phys. Soc. **51**, 340 (2006).

[19] W. Seka *et al.*, Phys. Plasmas **16**, 052701 (2009).

FIGURE CAPTIONS

FIG. 1. Color online (a) Schematic of target and beam irradiation showing the 900-μm-diam CD sphere with a re-entrant cone [Fig. 1(b)] that is irradiated with 36 OMEGA beams. The target and cone are filled with cryogenic liquid deuterium.

FIG. 2. Color online (a) VISAR data record (space versus time) with fringes that represent the velocity of the shocks produced by the laser pulse shown in the figure. The three shocks are observed as well as the jump in fringe position that occurs when the second and third shocks merge at 2.4 and 2.9 ns, respectively. (b) Streaked optical pyrometer (SOP) data showing the self-emission intensity (lineout in figure) follows the shock velocity and shock mergers providing corroboration of shock timing. (c) VISAR data for shot with lower second pulse and higher third pulse; these delay the first merger and advance the second, illustrating the technique to time shock in a tight sequence.

FIG. 3. Color online Inset: VISAR image for a four-shock experiment using an ICF drive pulse shown in figure. Three shocks are visible as in Fig. 2(a) with mergers at 1.6 and 2.3 ns. At 3.1 ns, the fourth shock (produced by the main pulse) overtakes them and soon after the flux from that shock causes the unshocked deuterium to absorb the VISAR laser.

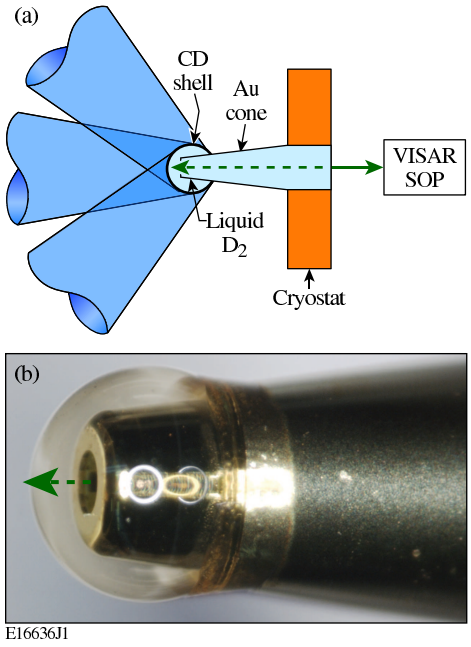

Figure 1 LB13021 17FEB2011

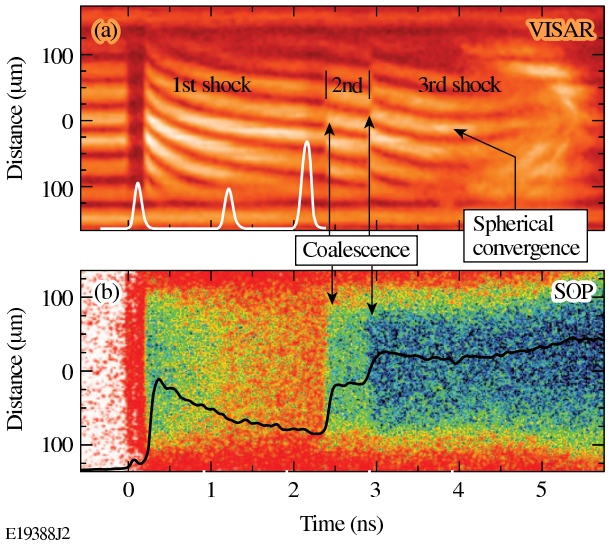

Figure 2 LB13021 17FEB2011

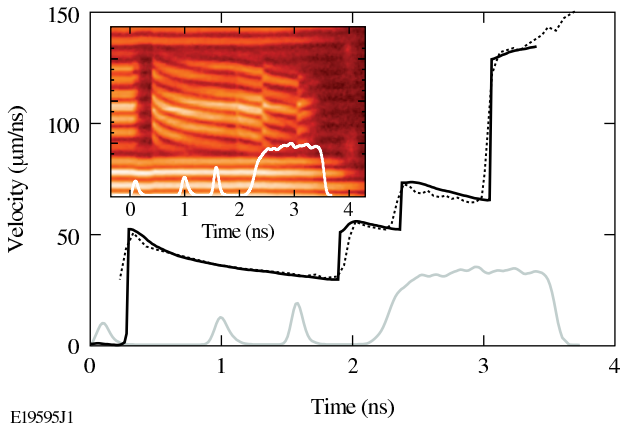

Figure 3 LB13021 17FEB2011